NASA/TM—2010-216897 AIAA–2010–7068

Loop Shaping Control Design for a Supersonic Propulsion System Model Using Quantitative Feedback Theory (QFT) Specifications and Bounds

Joseph W. Connolly and George Kopasakis
Glenn Research Center, Cleveland, Ohio

October 2010

NASA STI Program . . . in Profile

Since its founding, NASA has been dedicated to the advancement of aeronautics and space science. The NASA Scientific and Technical Information (STI) program plays a key part in helping NASA maintain this important role.

The NASA STI Program operates under the auspices of the Agency Chief Information Officer. It collects, organizes, provides for archiving, and disseminates NASA's STI. The NASA STI program provides access to the NASA Aeronautics and Space Database and its public interface, the NASA Technical Reports Server, thus providing one of the largest collections of aeronautical and space science STI in the world. Results are published in both non-NASA channels and by NASA in the NASA STI Report Series, which includes the following report types:

- TECHNICAL PUBLICATION. Reports of completed research or a major significant phase of research that present the results of NASA programs and include extensive data or theoretical analysis. Includes compilations of significant scientific and technical data and information deemed to be of continuing reference value. NASA counterpart of peer-reviewed formal professional papers but has less stringent limitations on manuscript length and extent of graphic presentations.

- TECHNICAL MEMORANDUM. Scientific and technical findings that are preliminary or of specialized interest, e.g., quick release reports, working papers, and bibliographies that contain minimal annotation. Does not contain extensive analysis.

- CONTRACTOR REPORT. Scientific and technical findings by NASA-sponsored contractors and grantees.

- CONFERENCE PUBLICATION. Collected papers from scientific and technical conferences, symposia, seminars, or other meetings sponsored or cosponsored by NASA.

- SPECIAL PUBLICATION. Scientific, technical, or historical information from NASA programs, projects, and missions, often concerned with subjects having substantial public interest.

- TECHNICAL TRANSLATION. English-language translations of foreign scientific and technical material pertinent to NASA's mission.

Specialized services also include creating custom thesauri, building customized databases, organizing and publishing research results.

For more information about the NASA STI program, see the following:

- Access the NASA STI program home page at *http://www.sti.nasa.gov*

- E-mail your question via the Internet to *help@sti.nasa.gov*

- Fax your question to the NASA STI Help Desk at 443–757–5803

- Telephone the NASA STI Help Desk at 443–757–5802

- Write to:
  NASA Center for AeroSpace Information (CASI)
  7115 Standard Drive
  Hanover, MD 21076–1320

NASA/TM—2010-216897 AIAA–2010–7068

Loop Shaping Control Design for a Supersonic Propulsion System Model Using Quantitative Feedback Theory (QFT) Specifications and Bounds

Joseph W. Connolly and George Kopasakis
Glenn Research Center, Cleveland, Ohio

Prepared for the
46th Joint Propulsion Conference and Exhibit
cosponsored by AIAA, ASME, SAE, and ASEE
Nashville, Tennessee, July 25–28, 2010

National Aeronautics and
Space Administration

Glenn Research Center
Cleveland, Ohio 44135

October 2010

Acknowledgments

The authors would like to express their gratitude to the Supersonics Project of the NASA Fundamental Aeronautics Program for supporting this reasearch effort. The aero-elastic modeling portion of this work would not have been possible without the assistance of Walt Silva, David Christhilf, and the rest of the Aero-Propulso-Servo-Elasticity team at the NASA Langley Research Center.

This work was sponsored by the Fundamental Aeronautics Program at the NASA Glenn Research Center.

Level of Review: This material has been technically reviewed by technical management.

Available from

NASA Center for Aerospace Information
7115 Standard Drive
Hanover, MD 21076–1320

National Technical Information Service
5301 Shawnee Road
Alexandria, VA 22312

Available electronically at http://gltrs.grc.nasa.gov

Loop Shaping Control Design for a Supersonic Propulsion System Model Using Quantitative Feedback Theory (QFT) Specifications and Bounds

Joseph W. Connolly and George Kopasakis
National Aeronautics and Space Administration
Glenn Research Center
Cleveland, Ohio 44135

Abstract

This paper covers the propulsion system component modeling and controls development of an integrated mixed compression inlet and turbojet engine that will be used for an overall vehicle Aero-Propulso-Servo-Elastic (APSE) model. Using previously created nonlinear component-level propulsion system models, a linear integrated propulsion system model and loop shaping control design have been developed. The design includes both inlet normal shock position control and jet engine rotor speed control for a potential supersonic commercial transport. A preliminary investigation of the impacts of the aero-elastic effects on the incoming flow field to the propulsion system are discussed, however, the focus here is on developing a methodology for the propulsion controls design that prevents unstart in the inlet and minimizes the thrust oscillation experienced by the vehicle. Quantitative Feedback Theory (QFT) specifications and bounds, and aspects of classical loop shaping are used in the control design process. Model uncertainty is incorporated in the design to address possible error in the system identification mapping of the nonlinear component models into the integrated linear model.

Nomenclature

2DB	Two-Dimensional Bifurcated inlet
A	Cross-sectional area
APSE	Aero-Propulso-Servo-Elasticity
C_{xy}	Coherence of x and y
CFD	Computational fluid dynamics
D	Magnitude drop in dB of U-contour
F_{source}	Friction addition
$G(s)$	Transfer function
GM	Gain margin
HSR	High Speed Research program
L	Atmospheric disturbance wave length
$L(s)$	Loop transmission function
LAPIN	Large Perturbation Inlet program
M	Mach number
M_p	Step response overshoot
M_{source}	Mass addition
P	Pressure
P_{xx}	Power spectral density of x
P_{xy}	Cross power spectral density of x and y
PM	Phase margin
Q_{source}	Heat addition
QFT	Quantitative Feedback Theory
R	Gas Constant

S^4T	Supersonic Semispan Transport
SISO	Single Input Single Output
T	Absolute temperature
T_{xy}	Complex data used to generate a transfer function
TDT	Transonic Dynamics Tunnel
V	Volume
$\dot{W}$	Mass flow rate
e	CFD internal energy term
j	Imaginary number
k	Transfer function gain
$\bar{q}$	Dynamic pressure
s	Laplace operator
t	Time
t_s	Settling time
u	Velocity
x	Length
Δ	Change in variable
δ_r	Difference in magnitude between upper and lower tracking bound as function of ω
ϵ	Atmospheric disturbance dissipation parameter
γ	Ratio of specific heat
λ	Excess number of poles to zeros
μ	Control parameter relating gain and phase margin
ρ	Density
σ	Pole representation for a transfer function
θ	Angle associated with phase margin
ω	Frequency
ω_n	Natural frequency
ζ	Damping ratio

Subscript

s	Static flow condition
t	Total flow condition
x	Input parameter
y	Output parameter

I. Introduction

UNDER the NASA Fundamental Aeronautics Program, the Supersonics Project aims to overcome the obstacles associated with supersonic commercial flight. The proposed vehicles are long, slim body aircraft with pronounced structural vibrations known as aero-servo-elastic modes.[1,2] When coupled with propulsion system dynamics, the modes are known as Aero-Propulso-Servo-Elasticity (APSE), and can potentially lead to design challenges that influence performance characteristics such as aircraft ride quality and stability. Other disturbances upstream of the inlet generated by atmospheric wind gusts, angle of attack, and yaw angle may also affect ride quality and stability. Work is currently on-going under this project to develop the technologies to allow for practical supersonic commercial flight at approximately Mach 2. To study the propulsion component of APSE, an integrated model is needed that includes both the inlet and engine propulsion system dynamics along with vehicle structural modes.

The supersonic inlet is of critical importance to the overall propulsion system as it is the first component that is exposed to the incoming flow field. The overall purpose of the inlet is to supply the engine with the required mass flow at the highest total pressure, while minimizing distortion. To meet the strenuous demands of supersonic flight above Mach 2, a mixed compression design is typically used in which the flow is compressed both external and internal to the inlet. The typical inlet thus resembles a convergent-divergent duct, where supersonic flow is primarily located in the convergent section and the subsonic flow is located in the divergent section, separated by a normal shock wave. The engine comprises the other major

component of the overall propulsion system and is connected just downstream of the inlet flow path. The engine models used for the control design build upon previous work with the General Electric J-85 and a generic medium bypass turbofan engine.[3,4] Currently, the model uses a single lumped volume for each of the major components, such as the compressor, combustor, turbine, and afterburner-nozzle. To study ride quality and stability, atmospheric turbulence models are used, based on work by Kopasakis,[5] to investigate their effect on the propulsion system.

The control design approach in this work comes from work in classical loop shaping by Kopasakis[6] and quantitative feedback theory (QFT) methodologies laid out by Houpis,[7] which account for design specifications in terms of bounds in a loop shaping development approach. The loop shaping approach presented here is a linear controls design methodology that requires the nonlinear propulsion models to be linearized prior to the development of control algorithms. This method is utilized for its ability to provide a structured approach while taking into account the transient response, stability, disturbance attenuation, and model uncertainty. While nearly any control design can be adjusted to account for uncertainty, QFT is a readily applicable methodology. The advancement over previous APSE work provided here for inlet-engine control design is the addition of uncertainty in the plant model and using aspects of classical loop shaping with QFT. The inclusion of uncertainty is critical as it helps to compensate for the potential errors in the system identification process and simplification assumptions in the model development, such as ignoring friction.

The overall APSE system schematic can be seen in Fig. 1. The core propulsion system of the overall model, highlighted in Fig. 1, is comprised of the linearized inlet, engine, and the propulsion controllers. All of the required flow elements are modeled using transfer functions, described in the following sections, to allow for the investigation of inlet normal shock movement and thrust oscillations. To start the simulation, free stream static conditions of pressure, temperature, and Mach number are applied to the inlet model. The inlet model then calculates the exit total pressure and temperature, all while controlling the normal shock position. Airflow properties at the inlet exit are used as the engine face input conditions establishing one of the propulsion system's boundary conditions that is required for the model. The engine then uses the input conditions to obtain exit flow properties that can be used to calculate the thrust, all while controlling the engine rotational speed. For a given operating condition, the speed of the engine can be related to the mass flow at the engine face through transfer functions. The mass flow at the engine input can act as an inlet exit plane disturbance, which will have an impact on the normal shock position due to the flow being subsonic. A transfer function is used to establish the relationship between the downstream mass flow and the normal shock position, allowing for the required feedback. The transfer functions used in the integrated propulsion model are for the cruise operating point indicating free stream conditions at 60,000 ft, Mach 2.35, and inlet exit airflow speed of Mach 0.45.

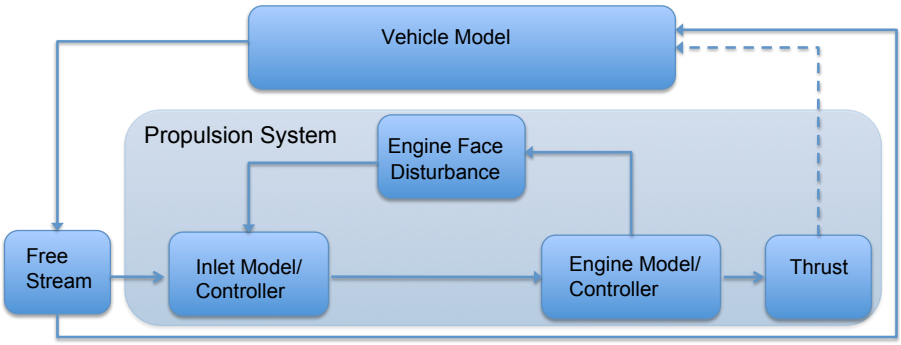

Figure 1. Schematic of overall APSE system model with propulsion system highlighted.

The incorporation of the vehicle model is still in a preliminary phase, however a simplified model is included that allows for free stream disturbances to perturb an aero-elastic model of the wing, which translate directly into additional free stream disturbances of the inlet. This is illustrated in Fig. 1, by the line from the vehicle model block to the free stream block. The part of the overall model still to be incorporated is the impact of thrust on the vehicle model. This is the dashed line from the thrust block to the vehicle model in Fig. 1. Currently the appropriate model of this feedback from the engine to the flexible vehicle model is still being developed and is not used in this preliminary model of the APSE system. The overall goal here is to eventually provide a high fidelity model for both the vehicle and propulsion system to investigate aero-elastic

effects. Previous work in the area of APSE has focused on either the vehicle or the propulsion system, but rarely both, unless being used in a hypersonic vehicle where the two systems are innately intertwined.[8–10] The paper layout starts with project background information, followed by inlet/ engine modeling and the establishment of the linear plants, outlines disturbance models, defines the aspects of QFT and classical control theory used, then outlines the proof of concept loop shaping process, and finally provides simulation results of the control design.

II. Analysis

A. Inlet Model

The overall purpose of the inlet is to supply the engine with the required mass flow with the highest pressure and least distortion. In the High Speed Research (HSR) program, a previous NASA supersonics program, several different types of inlets were investigated including a translating centerbody, variable-diameter centerbody, and a two-dimensional bifurcated (2DB) inlet.[11] The inlets were down-selected based on five metrics:

1. Inlet unstart probability
2. Inlet total pressure recovery
3. Inlet boundary layer bleed as a percent of inlet capture flow
4. Circumferential and radial inlet dynamic distortion
5. Inlet weight per unit airflow

In the end it was determined that the 2DB inlet, seen in Fig. 2, came closest to meeting all metrics, and this was the inlet chosen for this study. The inlet metric that is of paramount concern for safe flight operation is the inlet unstart probability, because unstart can cause sudden loss of thrust. Unstart refers to the normal shock, which separates the supersonic and subsonic flow internal to the inlet, being expelled outside of the inlet due to either upstream or downstream flow disturbances. For best performance, it is ideal to have the normal shock near the throat, which is the minimum cross-sectional area of the inlet. However, the normal shock is generally placed slightly downstream of the throat to increase stability. A basic sketch of the inlet shock wave pattern can be seen in Fig. 3. To avoid a catastrophic unstart, inlet bypass doors are used as control surfaces to manipulate the mass flow rate. The bypass door can be seen in Fig. 3 just before the engine face.

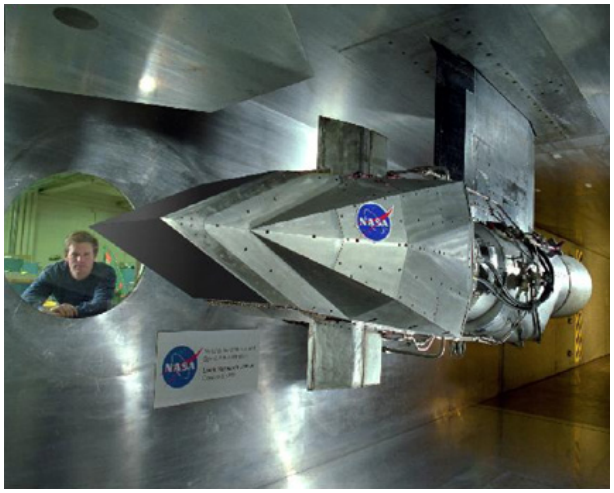

Figure 2. 2DB supersonic inlet attached to J-85 engine in NASA Glenn Research Center 10x10 supersonic wind tunnel.[12]

To model the complex dynamic behavior associated with the 2DB supersonic inlet, the Large Perturbation Inlet (LAPIN) flow code is used in this study.[13] LAPIN is a nonlinear, quasi-one-dimensional code capable of modeling the unstart phenomenon, inlet control parameters, and geometric variations. In order to meet the

needs of this work, the original Fortran source code was modified to adjust inputs and outputs for creating transfer functions. The linear inlet model was then used in the control algorithm development and the overall integration into a propulsion system model.

LAPIN uses quasi-one-dimensional Computational Fluid Dynamics (CFD) Euler equations to model the dynamic flow properties of the inlet. Quasi-one-dimensional means that the curvature of the duct is small in comparison to the passage diameter, allowing for the assumption that the fluid properties are uniform for a given cross sectional area of the inlet. A schematic of the modeling approach can be seen in Fig. 4 in which over a small distance, dx, the fluid properties change by a differential amount. In addition, LAPIN can allow for simple models of mass flow bleed as illustrated in Fig. 4. The bypass door is modeled as a bleed in LAPIN, as the main purpose of the bypass door is to adjust the mass flow through the inlet. The incorporation of the bypass/bleed model can be seen as a mass flow loss in Fig. 4. LAPIN assumes that the flow is thermally and calorically perfect, meaning the flow is governed by the ideal gas law seen in Eq. (1).

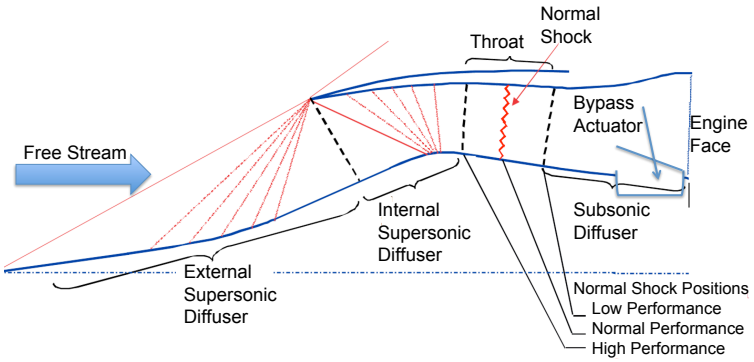

Figure 3. Supersonic inlet basic shock pattern.[14]

$$P = \rho RT \tag{1}$$

A brief synopsis of the LAPIN modeling approach is provided here. The detailed description of LAPIN is available in Varner.[13] The approach utilizes the conservation equations of continuity, momentum, and energy, Eqs. (2) to (4), respectively:

$$\frac{\partial(\rho A)}{\partial t} + \frac{\partial(\rho u A)}{\partial x} = M_{source} \tag{2}$$

$$\frac{\partial(\rho u A)}{\partial t} + \frac{\partial[A(\rho u^2 + P)]}{\partial x} = -P\frac{\partial A}{\partial x} + F_{source} \tag{3}$$

$$\frac{\partial[\rho(e + \frac{u^2}{2})A]}{\partial t} + \frac{\partial[Au(\rho(e + \frac{u^2}{2}) + P)]}{\partial x} = -P\frac{\partial A}{\partial t} + Q_{source} \tag{4}$$

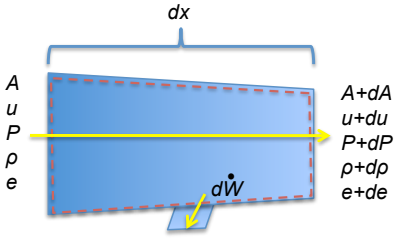

Figure 4. Quasi-one-dimensional flow representation of differential volume.

The governing equations can be thought of having source terms on the right hand side of the equation, thus allowing for the inclusion of models for bleed, bypasses, and inlet unstart/restart.

The 2DB inlet is modeled in LAPIN by dividing it into over a hundred volumes with the majority of the volumes in the supersonic portion of the inlet. The upstream flow properties are static pressure, temperature, and Mach number. The Mach number in the final modeled inlet volume is used for the downstream boundary condition. LAPIN is used here simply as a tool to generate data from which linear models can be computed, since the main concern of this study is the input, output, and coupling with other propulsion components. Therefore, the following flow variables: total pressure, total temperature, and shock position, are used to generate complex frequency data. A system identification process is then conducted to obtain the desired transfer functions. The process is the same for both the inlet and engine model and will be discussed in greater detail in the engine model section.

B. Engine Model

The engine comprises the other major component of the overall propulsion system, and is connected just downstream of the inlet flow path. Previous research from HSR looked into several engine designs and found that low bypass turbofan engines are desirable for this application.[15] The modeling effort here, however, will be for a turbojet engine similar to the General Electric J-85, due to a lack of detailed non-proprietary information for turbofan engines. The J-85 lends itself to a straightforward model development and verification because it has undergone extensive testing at NASA Glenn Research Center, has been used

in supersonic vehicles, and many of the required performance parameters are accessible. A basic schematic can be seen in Fig. 5. The primary purpose of modeling the engine is to obtain an accurate measure of the thrust that is needed to couple the propulsion system to the aero-servo-elastic model and assess the oscillations due to free stream disturbances.

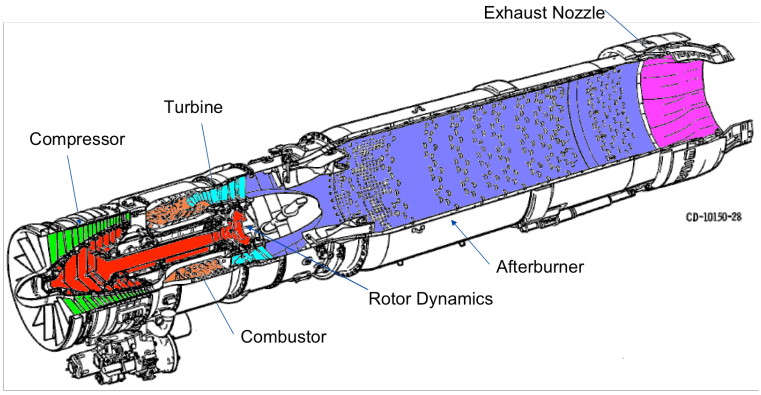

Figure 5. Schematic of turbojet engine.[4]

The model uses a single lumped volume for each of the major components such as compressor, combustor, turbine, afterburner, and nozzle. The modeling approach is outlined in Seldner[16] and refined in Kopasakis[4] and Stueber.[17] The high level equations are defined here for completeness and understanding the level of fidelity of the nonlinear simulation from which the linear engine model is ultimately developed and integrated into the overall propulsion model. Most of the geometric information for the engine is obtained from previous work done by Tesch.[18] Each of the fluid flow components is modeled using a set of derived conservation equations modified from the standard form and written in total condition form as continuity, momentum, and energy, Eqs. (5) to (7), respectively:

$$\frac{d}{dt}(\rho_s) = -\frac{1}{V}\Delta\dot{W} \tag{5}$$

$$\frac{d}{dt}(\dot{W}) = -\frac{A}{x}\Delta P_t \tag{6}$$

$$\frac{d}{dt}(\rho_s T_s) = -\frac{\gamma}{V}(T_t\dot{W}) \tag{7}$$

The three state variables chosen for the modeling of each component are the density, mass flow rate, and total temperature times density, which are tied together by the equation of state, Eq. (1). Since this is a subsonic system, two of the state variables must travel downstream, while the other travels upstream. Here the mass flow rate information travels upstream and the temperature and pressure travel downstream. A more detailed discussion can be found in Kopasakis.[4]

Linear Model Development

To develop an integrated model and design controllers, a linear model of the engine and inlet is required. The linearization is obtained from the nonlinear models by controlling the propulsion system to the desired cruise operating point and then simulating it as open loop. For this project, the goal for the engine is to control the thrust using the fuel flow rate into the combustor. Added fuel increases the energy of the flow, thus increasing the thrust. Sinusoidal sweeps are used to perturb the nonlinear models, allowing for the creation of transfer functions in a multi-step process over the relevant frequency range; a more detailed discussion can be found in Connolly.[3] A brief synopsis is provided here, starting with using Welch's average modified periodogram method.[19] The basic idea is simple in that one takes an input vector of data, x, and an output vector of data, y, and uses Welch's method to generate complex data as a function of frequency using the power spectral density as shown in Eq. (8). The x and y are used as subscripts in Eq. (8) and Eq. (9) to denote the input and output relation for each equation. To gauge how well this method estimates the actual dynamics, the coherence between the signals is computed in Eq. (9), where a value of one indicates a good representation, which provides valuable insight into the approximation.

$$T_{xy}(\omega) = \frac{P_{xy}(\omega)}{P_{xx}(\omega)} \tag{8}$$

$$C_{xy}(\omega) = \frac{|P_{xy}(\omega)|^2}{P_{xx}(\omega)P_{yy}(\omega)} \tag{9}$$

The expected dynamics that are of interest to this study are the flow perturbations induced by the atmosphere and vibrating airframe. The frequencies for these dynamics are assumed to be approximately 30 Hz for atmospheric disturbances and 50 Hz for aero-elastic disturances.[2] The sinusoidal frequency sweep used to generate the linear models is from a minimum frequency of 0.2 Hz to a maximum of 200 Hz. To gain a better understanding of the actual system identification approach, an inlet exit pressure disturbance will be used as an illustration. Figure 6 shows the logarithmic sinusoidal inlet exit pressure disturbance in the top subplot, and illustrates on the right hand y-axis the change in the disturbance frequency sweep over time, corresponding to the green line. The bottom plot is the corresponding open loop response of the speed of the engine spool.

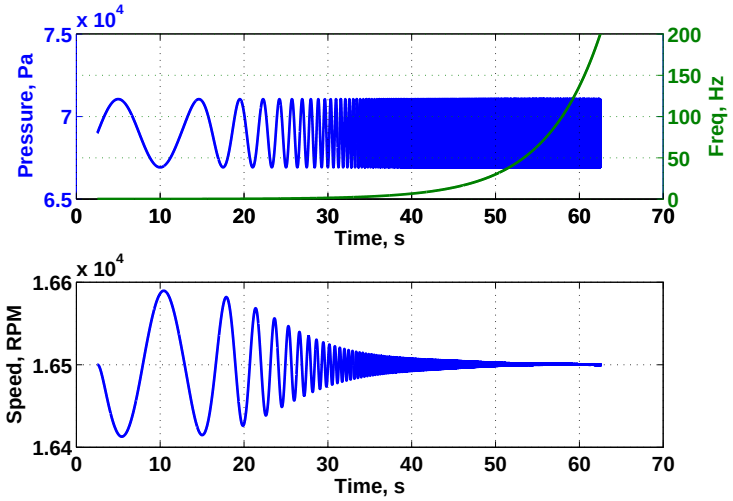

Figure 6. Inlet pressure logarithmic sinusoidal disturbance and frequency in top plot and engine shaft open loop speed response in lower plot.

Depicted in Fig. 7 (a) is a Bode plot of magnitude and phase, along with the coherence to ensure that the complex frequency data input and output signal are linearly related. The coherence shows that there is a strong correspondence between the input and the output vectors. This implies that the estimate using Welch's method is reasonable, with only a slightly lower coherence in the 1 Hz and below range. The transfer function estimate indicates that the linear model should have an adequate ability to model disturbances in the 30 to 50 Hz range.

Once the complex data as a function of frequency are obtained, a system identification procedure is used to generate the necessary poles and zeros of the transfer function that has the same frequency response as the complex data. This allows for implementation of the individual transfer functions into the integrated inlet-engine MATLAB® Simulink model. A detailed description of the system identification process can be found in Sugiyama.[20] A Bode plot of the transfer function is then compared with the Bode plots of the complex data, previously shown in Fig. 7 (a), to ensure an acceptable match. This is illustrated in Fig. 7 (b) for inlet exit pressure to spool rotational speed using a fourth order transfer function fit to the complex data.

For this operating point design, a transfer function model between second and eighth order is typically within a couple percent error when compared to the complex data. While the inlet exit pressure is used here to illustrate the approach, the same approach is used to obtain the linear models for the other relevant dynamics for the inlet and engine. However, a problem can arise utilizing this approach while developing a linear model. Some of the estimations of the resulting transfer function model can be of non-minimum

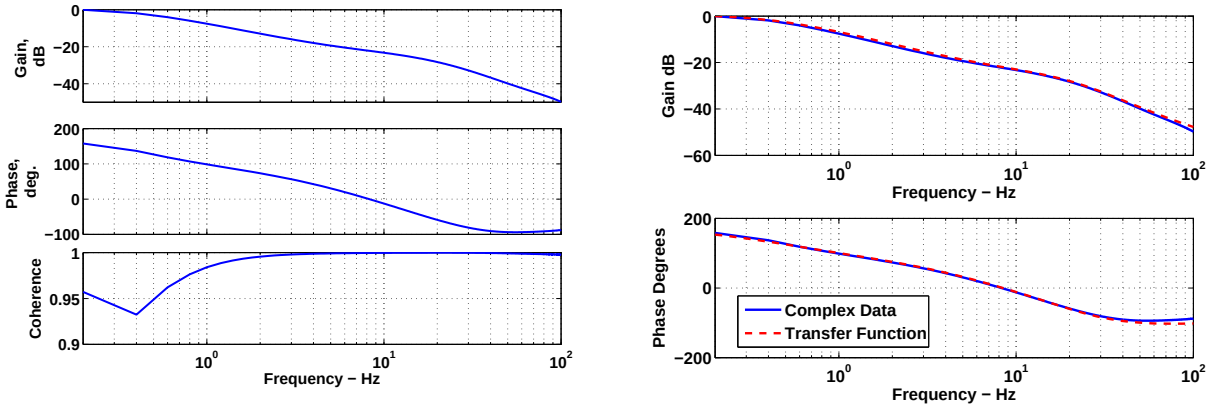

(a) Complex data

(b) Transfer function comparison

Figure 7. Inlet pressure to engine shaft speed frequency response using complex frequency data from Welch's method with coherence to ensure linear relationship (a). Inlet pressure to engine shaft speed Bode plot for complex data using Welch's method and 4th order transfer function obtained from system identification (b).

phase. This means that there is a phase offset from the actual plant due to zeros in the right half plane. Advancements in the QFT theory can deal with plants that are of non-minimum phase,[7] however, in general this type of plant creates problems for loop shaping control design.[6] As a result, the critical plants that produced non-minimum phase transfer functions were fitted by hand instead of using the system identification procedure.

C. Disturbance Models

In this control design, an important goal is to assess the worst possible disturbance that the plant is expected to encounter during operation. The proof of concept control design provided here investigates upstream flow disturbances caused by the atmosphere, and the effects of the aero-elastic model on the flow just upstream of the inlet. The atmospheric disturbance used here is considered severe, however there is no theoretical limit on how large a disturbance of this nature a vehicle can encounter. Some shortcomings of the current aero-elastic model are discussed below, as a clear worst case scenario for the model is still being defined. Due in part to current model limitations, the vehicle is perturbed at a transonic speed and at a lower altitude and thus higher dynamic pressure, instead of the cruise condition used for the rest of the study.

1. Atmospheric Models

The atmospheric model used here and outlined in more detail in Kopasakis[5,21] allows for practical and accurate time domain simulation of disturbances that are fractional order. This is accomplished by a combination of lead and lag transfer function estimations over the frequency range of interest. The resulting accuracy of the model is a function of the density of lead-lag filters used over each particular decade of frequency. The actual transfer function fits can be found in the appendix, Eqs. (18) to (21). A sum of sinusoidal disturbances is used as input to the atmospheric transfer functions over a prescribed range of frequencies. Given the cruise condition for a supersonic transport, the expected frequency range for moderate to severe turbulence is approximately 0.1 Hz to 35 Hz. The sum of sinusoids signal is then used to perturb four transfer functions representing different aspects of the atmospheric disturbance, namely the longitudinal, acoustic, pressure, and temperature. The longitudinal and acoustic transfer functions are directly related to a velocity disturbance, and the pressure and temperature transfer functions perturb the total pressure and temperature of the upstream flow field. Using upstream perturbations in LAPIN and the computed transfer functions, these atmospheric disturbances are then translated to disturbances in the normal shock position.

2. Aero-elastic Models

The aero-elastic vehicle model used here was developed by NASA Langley Research Center from test data generated using the Supersonic Semispan Transport (S^4T) in the Transonic Dynamics Tunnel (TDT). The TDT was specifically built to investigate flutter, which is an aero-elastic effect where the vehicle's wing oscillates violently and can cause major structural damage. A schematic of the S^4T can be seen in Fig. 8, where the model is a flexible representation of half of a supersonic civil transport. The test data allowed for the

creation of numerous linear models at test conditions ranging from Mach 0.6 to 1.2 and dynamic pressure, $\bar{q}$, from 0 to 250 lbs/ft^2. At each condition the model allows for inputs of vehicle flight controls and atmospheric wind gusts, and the resulting acceleration of the S^4T model is measured at various locations. The operating condition of the linear vehicle model chosen for this study was at Mach 1.2 and the highest possible $\bar{q}$ while avoiding a full flutter condition, which was 115 lbs/ft^2. For the purposes of this study, it was assumed that there is no flight control and as such the flutter condition would result in an unstable plant model. Given the assumption of no flight control, the disturbances are more of a worst case in the sense they are not dampened out, but it is also not the most severe condition the vehicle may be able to handle if a flight control is used. The primary input of interest for the development of the model in this study is the atmospheric wind gust, and the output of interest is the acceleration at the sensor location at the wing tip for the underhung engine furthest from the fuselage, shown in Fig. 8.

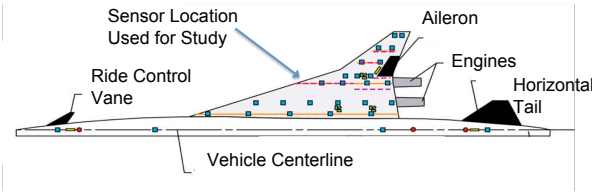

Figure 8. Top view of the S^4T model schematic with blue squares representing sensor locations.[2]

An atmospheric velocity disturbance, discussed above, serves as the model input, which results in a wind gust that excites vertical accelerations of the wing tip above the propulsion system inlet. This acceleration is then integrated and directly translated into an additional free stream velocity disturbance at the inlet. Two major shortcomings currently exist for this model. First, the additional velocity disturbance is directly translated to the inlet face, meaning it is propagated with no delay or dissipation. This could be acceptable for a first cut given that this is for a demonstration control design and the test case is really a worst case scenario. The other shortcoming is that the model is currently only valid for up to Mach 1.2 and not the cruise condition of the vehicle, Mach 2.35. This could produce significant error, however current thought is that the transonic phase of flight could produce the most severe conditions for flutter due to the abrupt shock formation across the wing. Also, the higher dynamic pressure could cause greater forces than those experienced at a cruise altitude. This will need to be investigated further and will be addressed in future work.

D. Controller

The control design presented in this paper is for a proof of concept, and uses aspects of classical loop shaping[6] design and QFT.[22] The classic design allows for easier inspection of the impacts of the actuator bandwidth and disturbance attenuation, whereas QFT can directly account for uncertainty in plant dynamics.[7] A controller is developed for both the engine rotational speed and the inlet normal shock position, both of which result in a single input single output (SISO) design. As in any control design, it is key to understand the expected disturbances and main objectives of the controlled system. For this study it is critical to attenuate disturbances in the tens of hertz corresponding to the atmospheric and aero-elastic effects. In general, a fuel injector for a commercial turbojet/turbofan engine has a bandwidth of approximately 10 Hz, thus it will not be able to attenuate disturbances in the tens of hertz. This results in the inlet bypass door, with a bandwidth of approximately 200 Hz, being the primary means to attenuate the higher frequency disturbances and reduce thrust oscillations. For brevity, the approach of the control design method will be explained for the particular case of the inlet control, however both designs are critical for proper propulsion system operation.

QFT is a frequency domain technique that quantitatively formulates the uncertainty of a plant model, allowing for the design of feedback control. The main advantage of QFT is that it is an established methodology that allows for the development of a single controller to handle all possible plants defined by the space of uncertainty. This is accomplished by defining discrete test cases of plants, as will be discussed in more detail below. All of the individual plants are continuous, time invariant SISO models, defined by the uncertainty specified in the design. A nominal plant is chosen from all possible plants by inspection of the templates. The templates illustrate the variation in output magnitude and phase response at a specific frequency, caused by the uncertainty in plant model parameters. This is an important point, because if uncertainty were ignored, then the template would be a single point, and control designs that do not allow for sufficient margin could result in actuator saturation or instabilities. The plot of QFT performance is typically done on a Nichols chart, which combines the two plots typically seen in a Bode plot. In the Nichols chart, the x-axis is phase,

the y-axis is magnitude, and each data point pertains to a specific frequency. This chart is very helpful for visualizing the loop transmission to be discussed below, but can also provide information about the closed loop frequency response data or the M-contours, by overlaying these contours on the Nichols chart.

The proof of concept control design uses four main parameters to investigate performance. The first and most critical is stability, which will be defined using the QFT U-contour. The contour provides a region on the Nichols chart that the control design must not enter. Next, the disturbance attenuation and limit of the actuator bandwidth is illustrated using classical methods of a proposed desirable loop transmission. Finally, tracking bounds are designed using QFT.

The first step in the QFT design process is to define the expected uncertainty in the plant model of the inlet bypass door movement to normal shock position, provided in appendix, Eq. (24). The major sources of uncertainty in the inlet plant are the possible errors introduced in the system identification process and possible errors in the capturing of the normal shock position with a relatively simple quasi-one dimensional CFD approach. Given this, an error of $\pm 20\%$ was assumed to the gain of the plant model and the lowest frequency pole. The region of plant parameter uncertainty can be seen as the shaded area in Fig. 9. Each of the red circles represent a different plant based on variations of the gain and lowest frequency pole. The entire shaded region represents the uncertainty, however only the individual test cases are required for the QFT design.

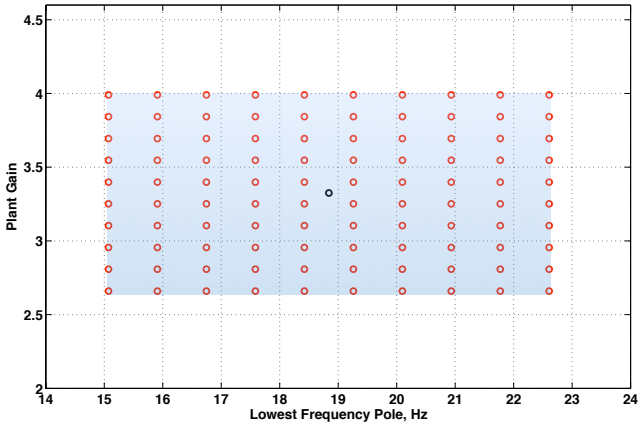

Figure 9. Region of plant parameter uncertainty for lowest frequency pole and gain shown in shaded region, individual plants as red circles, and original plant as black circle.

The next step in the design process is to determine a relevant discrete set of frequencies for which to inspect the uncertainty in the design process. As a general rule, at least one frequency point should be chosen per decade over the relevant bandwidth. Once the plant uncertainty and frequencies of interest are determined, plots of the plant templates can be obtained, which provide the possible error of the plant in magnitude and phase at a given frequency. The plant templates consist of both the plant and the actuator, $G(s)_{overall,plant} = G(s)_{actuator}G(s)_{plant}$. One of the key aspects of the templates is that, in most cases, the extremes of the uncertain parameters (retangular edge point of Fig. 9) constitute the exterior points of the template. When this is the case, only these points need to be carried forward in the design, which can greatly reduce the number of calculations required, otherwise every combination of the uncertain parameters would need to be calculated at each step of the design. Templates also in general collapse to a straight line as the frequency increases. This will become important later in the development of the stability bounds. An example template for $\omega = 1$ Hz can be seen in Fig. 10, where the red + symbols represent the extreme points of the uncertain parameters.

In any loop shaping design, the main goal is to shape the loop transmission, Eq. (10), to meet a desired control performance goal.

$$L(s) = G(s)_{control}G(s)_{actuator}G(s)_{plant} \tag{10}$$

This is related to the closed loop system response in a unity feedback back design. One can use the classical loop shaping method using the loop transmission to provide insight into a desirable control design. The

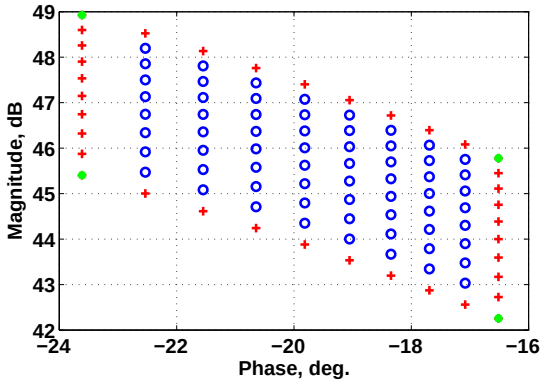

Figure 10. Plant uncertainty template at a frequency of 1 Hz, all points represent individual plant models, with exterior points corresponding to exterior points from Fig. 9.

description of a desirable loop transmission is detailed in Kopasakis,[6] and will be used here to provide a guide of the desired disturbance attenuation. A desirable loop transmission will have a higher gain in the lower frequency range, while ensuring that the bandwidth, or zero decibel crossover frequency, occurs at the limit of the actuator capabilities. The higher gain will allow for disturbance attenuation in the lower frequencies,

$$attenuation \approx 10^{\frac{Magnitude(dB)}{20}}$$

while not exceeding bandwidth restrictions. A loop transmission function to meet this objective is easily constructed using poles and zeros and the desirable loop transmission Bode plot can be seen in Fig. 11. While the QFT design illustrates bounds and regions of instability, it can lack that clear goal of what a proper design should resemble to assist a controls engineer with limited experience. By integrating aspects of the classical approach, the designer has additional tools to guide the design when moving from a Bode representation of the loop transmission function to the typically used Nichols chart utilized by QFT.

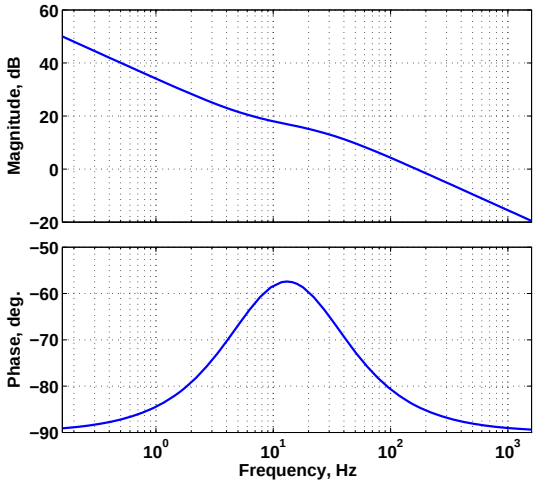

Figure 11. Bode plot of a desirable loop transmission response to establish expected disturbance attenuation.

The next step is to obtain the U-contour or the region of instability on the Nichols chart. The stability goal for this design is a phase margin of 60°. Given that the Phase Margin (PM) can be given by Eq. (11), rearranging can provide θ.

$$PM \geq 180^o - \theta \tag{11}$$

This can then be plugged into Eq. (12) to provide μ and thus the relation from PM to Gain Margin (GM) is obtained from Eq. (13). This provides the necessary information to realize the stability bound on the Nichols chart without consideration of uncertainty.

$$\theta = 2cos^{-1}(\frac{0.5}{\mu}) \in [0, 180] \tag{12}$$

$$GM \geq 1 + \frac{1}{\mu} \tag{13}$$

Given that the plant templates approximate a line as the frequency of the template increases, the plant can be approximated by Eq. (14), where λ is the number of excess poles in comparison to zeros.[7] This results in the variability of the uncertain plant only having an impact from the change in gain. Therefore the change in the U-contour to account for the plant uncertainty is simply obtained by Eq. (15).

$$\lim_{\omega \to \infty} [G_{overall,plant}(j\omega)] = \frac{k}{\omega^{\lambda}} \tag{14}$$

$$D = 20 \log_{10}(k_{max} - k_{min}) \tag{15}$$

The obtained value then lowers the lower portion of the stability ellipse to form a U-contour shown in red in Fig. 12, with the the desirable nominal loop shape, from Fig. 15, in blue. Recall, it is the objective to avoid entering the U-contour. This provides a minimum set of guidelines for a stable system with the ability to obtain a margin of disturbance attenuation. In most designs though, it is desired to have a specified ability to track a reference command. This is a critical problem in the inlet control design to avoid an unstart condition.

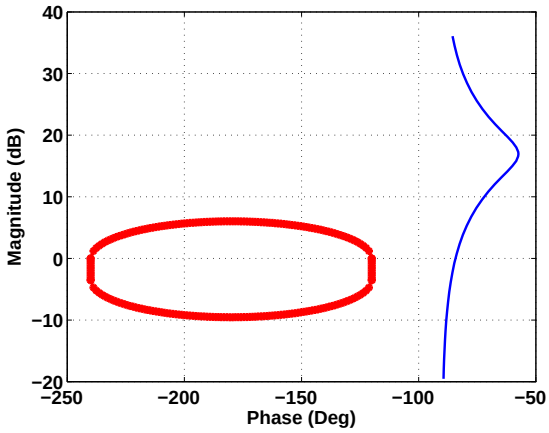

Figure 12. Nichols chart of the U-contour (red) and the desired open loop response (blue).

The tracking bounds for this design will be assumed for demonstration purposes as a restriction on the overshoot, $M_p = 4\%$, and settling time, $t_s = 0.0045$ s, for a given upper bound in the time domain, while the lower bound is defined as $M_p = 0.002\%$ and $t_s = 0.025$ s. An added specification of the tracking bounds is that the upper bound has a bandwidth equal to that of the actuator limit. Given the specification, the following second order approximations can be used to obtain the transfer functions that bound the desired response: $M_p = e^{\frac{-\pi\zeta}{\sqrt{1-\zeta^2}}}$ and $t_s = \frac{4.6}{\sigma}$, where $\sigma = \zeta\omega_n$. The transfer functions of the upper and lower bound then typically take the shape of Eq. (16) and Eq. (17), respectively.

$$T_{RU}(s) = \frac{\omega_n^2}{s^2 + 2\zeta\omega_n s + \omega_n^2} \tag{16}$$

$$T_{RL}(s) = \frac{k}{(s - pole_1)(s - pole_2)} \tag{17}$$

The goal of the tracking bounds is to have the upper and lower bounds continuously diverge in magnitude from one another as a function of increasing frequency as shown in Fig. 13 (a). This is required for implementation

of the QFT tracking bounds. The monotonically increasing difference in decibels is defined as δ_r. The divergence can be seen in Fig. 13 (b). If δ_r is not monotonically increasing, adjustments to Eq. (16) and Eq. (17) can be made by increasing the number of poles or zeros of the transfer functions.

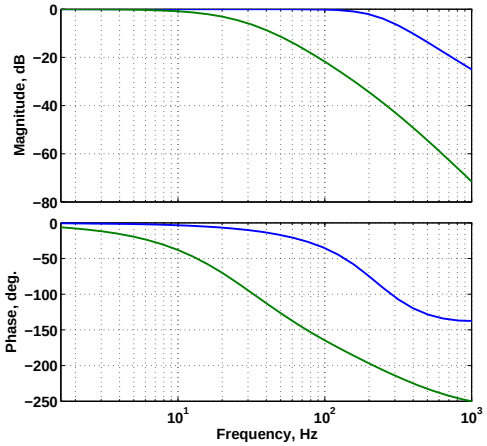

(a) Bode Plot

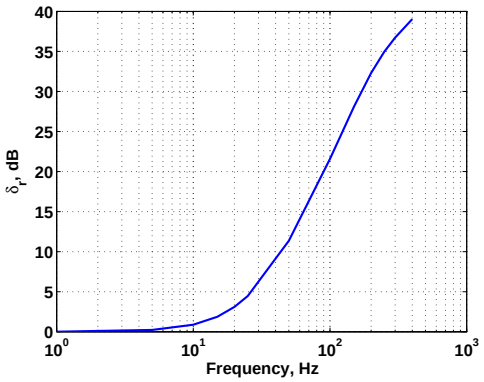

(b) δ_f

Figure 13. Bode plot of the upper and lower tracking bounds, illustrating the diverging magnitude as frequency increases (a). Plot of the δ_r function showing the increasing magnitude as frequency increases (b).

Now that the tracking bounds are known, we can again go back to the plant templates to account for the uncertainty while using the tracking bounds for the QFT design. Looking back at Fig. 10, the four extreme points of the plant uncertainty are plotted as green dots. While each point represents a different plant given a prescribed uncertainty, one of these four corners is typically used as the nominal plant; in this case, the point of lowest magnitude is chosen. The notion of the nominal plant in QFT is what allows for a single loop shaping design to account for the many plants that make up the space of the uncertainty. All of the QFT bounds, even those beyond the scope of this paper, use the nominal plant to create limits on the Nichols chart that account for the variability of the chosen nominal plant.[7] The steps to obtain the tracking bounds are listed below; more detail can be found in Houpis.[7]

1. Obtain δ_r
2. Select a nominal plant, typically the lowest magnitude plant from a given template
3. At a given frequency, line up the template's lowest phase side at -90°
4. Given the M-contours of constant closed loop magnitude, move the template up and down in magnitude until the difference between the highest and lowest magnitude points of the template match that of δ_r at the chosen frequency of the template.
5. Repeat the above process for increasingly negative phase values, -100°,-110°,$\cdots$, until the stability boundary is crossed.
6. Repeat the entire process for each frequency of interest.

Once the tracking bounds are obtained at each frequency of interest, the goal is to have the loop transmission at the corresponding frequencies above the obtained bound.The complete bounds are shown in Fig. 14 with the U-contour in red, the tracking bounds as the various colored horizontal lines, desirable loop transmission in dashed green, and the achieved loop transmission is in black. The shaping of the nominal plant loop transmission is conducted by constructing the controller with the required poles and zeros. While the loop transmission comes close to the U-contour, it does not cross and thus each of the plants should have approximately 60° of phase margin. The tracking bounds are used to check that the loop transmission magnitude at a specified frequency is above the tracking bound. The colored circles in Fig. 14 correspond to each of the frequencies at which the colored tracking bounds are plotted. Tracking specifications in this design were too strict given the amount of uncertainty in the plant. Thus, in the lower frequencies, the loop

transmission may not achieve the tracking objective for all plants because the plotted circles are not above their respective bound. In a control design to be implemented for hardware, this would be the point at which the control designer would investigate multiple control designs, discuss the loosening of tracking specifications, or the tightening of the uncertainty in the plant model by higher fidelity models, or the possibility of increasing the bandwidth of the actuator.

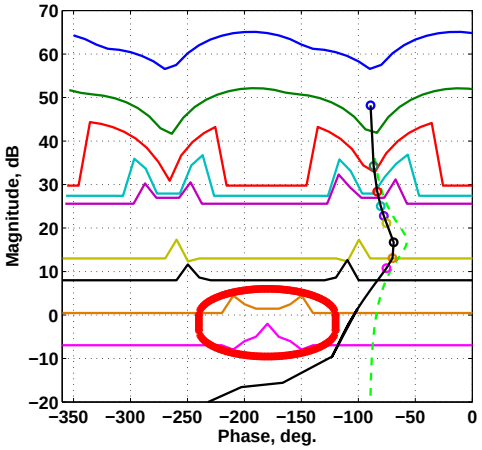

Figure 14. Nichols diagram of the QFT bounds: U-contour (in red), tracking bounds (as various colored horizontal lines), desirable loop transmission (dashed green line) and the achieved loop transmission (black line).

As a check to investigate the performance over the entire space of uncertainty, shown in Fig. 9, a step response of each corresponding plant is plotted in Fig. 15 (a), with the overlay of the upper and lower tracking bounds in dashed red lines. This illustrates a reasonable control design for a preliminary investigation, but it can be seen that in the initial transient, the response is approximately on the bound, and as the response settles, the lower bound is stricter than the achieved performance. The relative fast initial time response is indicative of a high bandwidth controls design, followed by a slower response until the system settles that is due to the lowest frequency zero in the controls design. Referring to the loop transmission shape design shown in Fig. 15 (b), this type of controls design helps to insure a high bandwidth (fast response), with sufficient stability margins, and high mid-frequency disturbance attenuation.

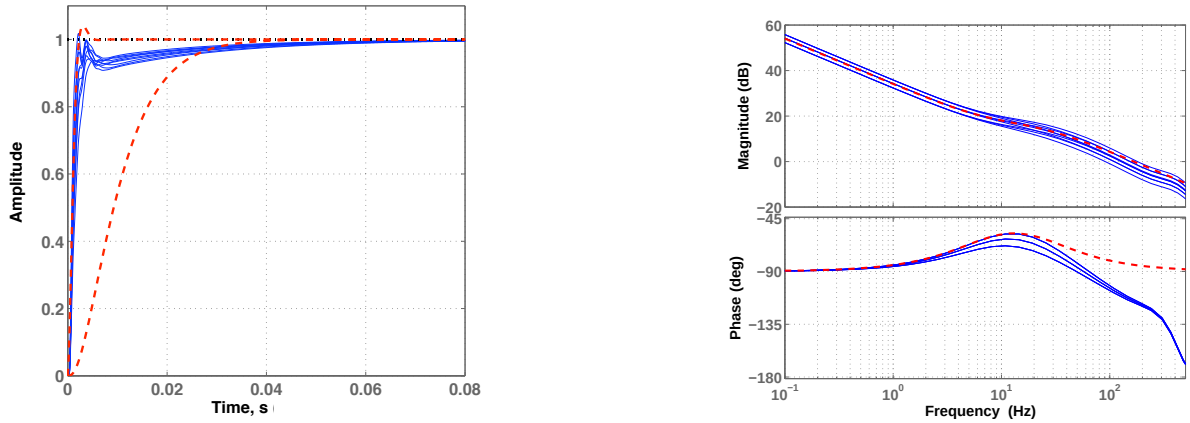

(a) Step

(b) Bode

Figure 15. Step response of all plant uncertainties (blue lines) and the desired tracking bounds (red dashed lines) (a). Loop transmission bode plot of all plant uncertainties (blue lines) and the desirable loop transmission response to establish disturbance attenuation (red dashed line) (b).

The final check of the design is to ensure that the primary goal of disturbance attenuation is obtained and that the actuator bandwidth is not exceeded. This is easily done in a classical approach using the Bode plot, shown in Fig. 15 (b). The desirable loop transmission is plotted in dashed red and it can be seen that all of the plants have a bandwidth of 200 Hz or less, therefore the actuator limits are preserved. The Bode plot also allows for easy inspection of the attenuation by the magnitude above zero in the lower frequencies. This design provides the expected attenuation factor of approximately 10 times at 10 Hz, based on the desired loop transmisison. Even with the uncertainty in the plant model, this control design will be able to provide some disturbance attenuation up until 190 Hz, as this is the point at which the worst loop transmission crosses the zero decibel line. The final controller transfer function can be found in the appendix, Eq. (24).

A similar control design is conducted for the rotational speed of the engine using a fuel flow injector. The related transfer functions of the design are provided in the appendix, Eqs. (25) to (27). For the remainder of the paper, the disturbances investigated will be of a higher frequency than the fuel injector, thus it is not expected that the fuel injector will have a high enough bandwidth to effectively contribute to the disturbance attenuation.

III. Results

Upon completion of the linear model development and controller design, all of the transfer functions are assembled into an overall propulsion system model and preliminary APSE model in the Simulink environment. The vehicle portion of the model is still considered preliminary, because the thrust feedback to the vehicle is not modeled. The linear model is developed at a supersonic cruise of Mach 2.35 and an altitude of 60,000 ft. The turbulence rating for this atmospheric model is considered severe. The atmospheric models produce a velocity, pressure, and temperature disturbance, of which the velocity disturbance can be seen on the left hand side of Fig. 16. This velocity disturbance is then fed into the aero-elastic model, which from wing velocity disturbances introduces an additional velocity disturbance, shown in Fig. 16, right hand side. The two signals are then combined into an overall disturbance. It is obvious that the atmospheric disturbance has the greater magnitude, and is the dominant concern for attenuation.

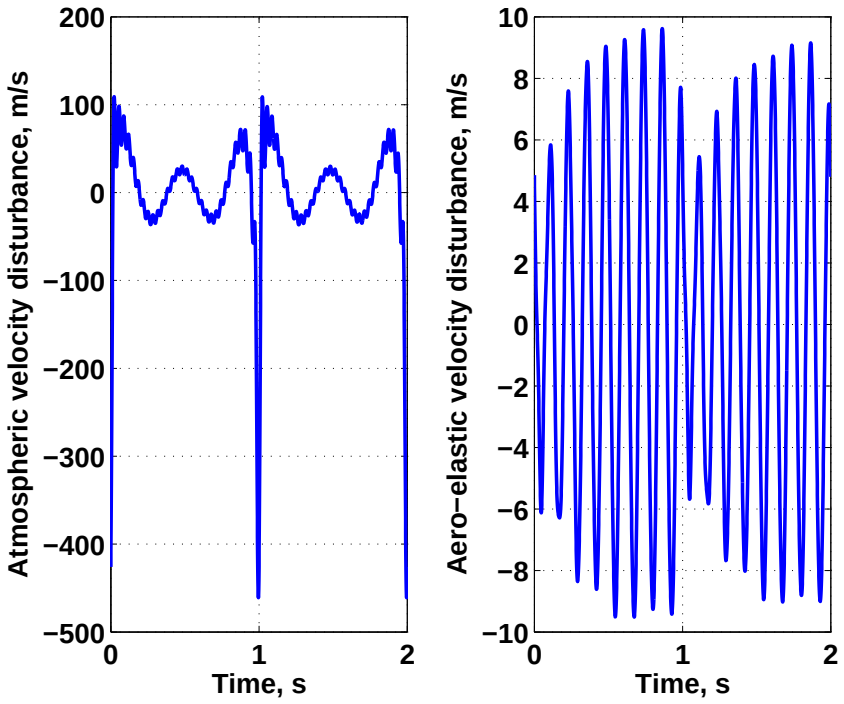

Figure 16. Atmospheric disturbance translated to velocity and additional velocity disturbance component from aero-elastic effects.

These disturbances are then fed into the transfer functions described earlier, defined by Eqs. (22) to (27), to create an overall disturbance to the normal shock position, which is attenuated by the controller. Both

the open loop and closed loop response about the nominal normal shock location in the inlet can be seen in Fig. 17 (a). In this example, the bypass door controller is able to attenuate the disturbances of the larger disturbance spikes that almost resemble an impulse signal.

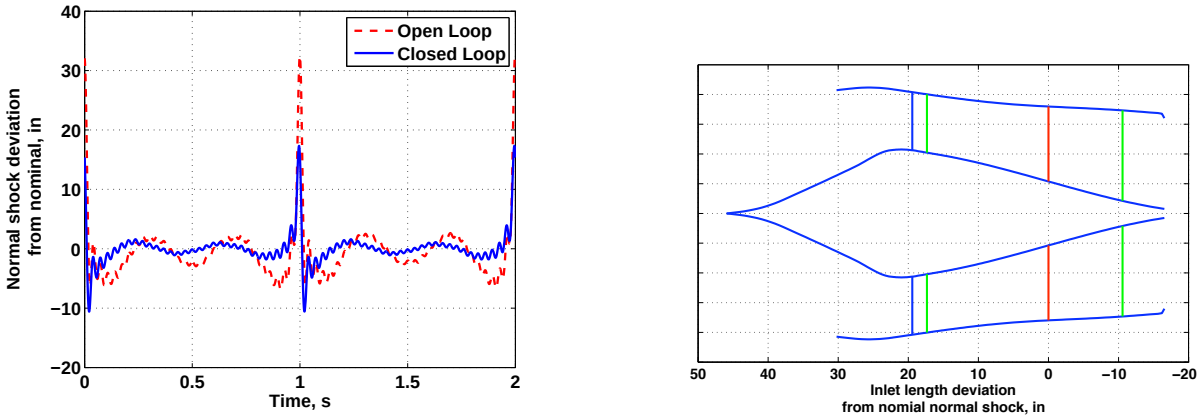

(a) Open and closed loop shock position response

(b) Shock position response in relation to unstart

Figure 17. Open loop and closed loop normal shock response to atmospheric and aero-elastic disturbances (a). Inlet with nominal shock location in red, geometric throat in blue, and maximum closed loop movement of shock in green (b).

As can be seen, the normal shock moves approximately 17.5 in from its designed operating position instead of the possible 33 in if the disturbance were uncontrolled. To illustrate the importance of the bypass door controller, the inlet key shock locations are plotted in Fig. 17 (b). The nominal shock position is in red, the maximum movement of the shock is shown in green. The shock does move forward in the inlet, but it avoids crossing the geometric throat of the inlet shown in blue. If the bypass door controller had not been used, the magnitude of the open loop shock movement would result in an inlet unstart condition, as the shock would have crossed the geometric throat.

The shock position is related to a pressure and temperate disturbance at the engine face, resulting in engine speed fluctuations. Given that the inlet control dampens out what would be otherwise the open loop pressure and temperature disturbance at the engine face, the engine controller is able to handle small fluctuations in the rotational speed. The small fluctuations in the rotational speed correspond to small changes in the thrust, due to the change in fuel flow.

Changes in the fuel flow also cause perturbations at the engine face, which are accounted for as inlet downstream perturbations to complete the feedback system for the propulsion system portion of the model. The resulting thrust oscillations can be seen in Fig. 18. The magnitude of the oscillations is relatively small, only a couple percent change from nominal, but much of this analysis is still preliminary and a further study is required to say anything definitive.

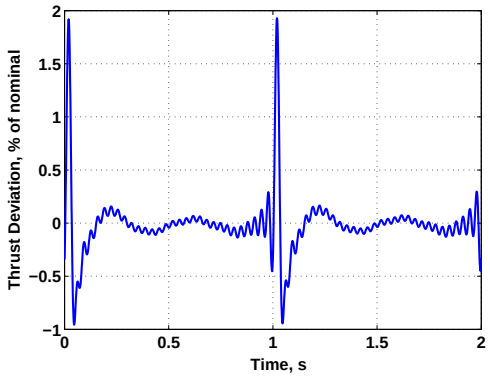

Figure 18. Closed loop thrust oscillation as percent of nominal thrust

IV. Future Work

Future work in this area includes current efforts in the development of a nonlinear inlet model that is conducive for testing the control algorithms on an integrated nonlinear model. The linear model can still serve as a controls development environment, but a more rigorous verification should be done using nonlinear models. Improved fidelity of the engine model to investigate surge and rotating stall could be added to allow for a further understanding of the impacts of events that could result in an inlet unstart. While the controls approach here is very helpful in relating performance specifications to the actual design procedure, some automation of the process of obtaining transfer functions that currently need to be completed by hand could make this a very powerful tool. Finally, additional integration with the airframe dynamics model developed by NASA Langley Research Center is required to move beyond a preliminary model, thus allowing for implementation of the thrust feedback and operating condition matching.

V. Conclusion

In this paper, an integrated linear propulsion system model about the cruise operating point with Quantitative Feedback Theory (QFT) controls design is presented, allowing for preliminarily investigation of thrust oscillations. The control algorithms here are not optimized, as the exact design of the propulsion system to be used is still being determined. However, a process for designing an inlet controller was shown, which attenuated incoming flow field perturbations thereby preventing an inlet unstart condition. A preliminary inspection of a linear integrated Aero-Propulso-Servo-Elasticity (APSE) model was conducted, by incorporating the aero-elastic effects into the flow field disturbances. Currently the thrust oscillation feeding back to the vehicle is neglected, but a method for developing the complete integrated model was illustrated. The goal here was to illustrate an approach to solve the problem of dynamic thrust oscillations and to show its feasibility in obtaining realistic results.

Preliminary results here show that developing controllers for a linear propulsion system model about the cruise condition can give reasonable disturbance attenuation of atmospheric and representative aero-elastic disturbances to limit the amount of thrust oscillation. The loop shaping approach, using both classical and QFT controls methods, has been shown to provide valuable insight to the design process. The amount of attenuation ultimately required for the flow field disturbances will need to be defined as more information becomes available and designs are finalized. This could alter the design presented here. However, this approach provides a reasonable solution and allows for easy adaptation as the project matures.

Appendix

Model Transfer Functions

The first set of equations in the appendix is for the atmospheric disturbances, Eqs. (18) to (21), temperature, pressure, longitudinal, and acoustic, respectively.

$$G(s)_{atmo,T} = 3.74\epsilon^{\frac{2}{6}} L^{\frac{5}{9}} \frac{(s/33+1)(s/45.6+1)(s/602.4+1)}{(s/1.1+1)(s/25.1+1)(s/109.8+1)(s/816.3+1)} \tag{18}$$

$$G(s)_{atmo,P} = 3.4\epsilon^{\frac{2}{6}} L^{\frac{5}{6}} \frac{(s/33+1)(s/45.6+1)(s/602.4+1)}{(s/1.1+1)(s/25.1+1)(s/109.8+1)(s/816.3+1)} \tag{19}$$

$$G(s)_{atmo,long} = 1.75\epsilon^{\frac{2}{9}} L^{\frac{5}{9}} \frac{(s/9.2+1)(s/55+1)(s/335.5+1)}{(s/1.46+1)(s/30.1+1)(s/85.7+1)(s/1593+1)} \tag{20}$$

$$G(s)_{atmo,acoustic} = 1.87\epsilon^{\frac{2}{6}} L^{\frac{5}{6}} \frac{M\gamma R}{a_o} \frac{(s/33+1)(s/45.6+1)(s/602.4+1)}{(s/1.1+1)(s/25.1+1)(s/109.8+1)(s/816.3+1)} \tag{21}$$

The development of these equations can be found in Kopasakis.[5] One variation from previously developed equations is the severity of the turbulence. The disturbances presented here are considered severe, and thus the eddy disipation, ϵ is larger, 0.778×10^{-3}, however the length, L, remains constant at 765 meters.

The inlet model transfer functions are shown as Eqs. (22) to (24), inlet actuator model, inlet plant model, and inlet controller, respectively. A QFT design process for the normal shock position can be conducted using these transfer functions.

$$G(s)_{inlet,actuator} = \frac{3.8949e14(s+1571)(s+62.83)}{(s+2.195e4)(s+59.85)(s^2+1800s+1.409e6)(s^2+1941s+2.076e7)} \tag{22}$$

$$G(s)_{inlet,plant} = \frac{3.0221e31(s+2513)(s+653.5)}{(s+118.4)(s^2+1348s+8.3e5)(s^2+4362s+1.109e7)(s^2+3456s+9.87e6)\cdots (s^2+4609s+1.238e7)(s^2+4856s+1.374e7)} \quad (23)$$

$$Num(s) = 9.5453e14(s+1257)(s+118.4)(s+45)(s^2+1275s+8.3e5)(s^2+2199s+2.467e6)\cdots (s^2+3534s+5.552e6)(s^2+2419s+1.194e7)(s^2+1188s+1.567e7)$$

$$Den(s) = s(s+785.4)(s+653.5)(s+150)(s^2+5.454e4s+1.518e9)(s^2+5.63e4s+1.617e9)\cdots (s^2+5.806e4s+1.72e9)(s^2+5.982e4s+1.825e9)(s^2+6.158e4s+1.934e9)$$

$$G(s)_{inlet,controller} = \frac{Num(s)}{Den(s)} \quad (24)$$

While the engine control design was not specifically discussed in this paper the model transfer functions and controller are given for completeness in developing the integrated propulsion model. The engine model transfer functions are shown as Eqs. (25) to (27), engine actuator model, engine plant model, and engine controller, respectively. A QFT design process for the rotor speed can be conducted using these transfer functions for investigation of thrust oscillations.

$$G(s)_{engine,actuator} = \frac{1421}{s^2+52.78s+2842} \quad (25)$$

$$G(s)_{engine,plant} = \frac{6.1136e17(s+111.8)}{(s+345.6)(s+13.82)(s^2+1004s+5.041e5)(s^2+1153s+5.317e6)} \quad (26)$$

$$G(s)_{engine,controller} = \frac{3.4361(s+63.77)(s+0.6283)(s^2+59.28s+1216)}{s(s+9.425)(s^2+4398s+9.87e6)} \quad (27)$$

References

[1]Cohen, P., Long-Davis, M., and Povinelli, L., "Fundamental Aeronautics Program - Supersonics Project," http://www.aeronautics.nasa.gov/fap/documents.html, 2006.

[2]Perry, B., Silva, W., Florance, J., Wieseman, C., Potozky, A., Sanetrik, M., Scott, R., Keller, D., Cole, S., and Coulson, D., "Plans and Status of Wind Tunnel Testing Employing an Aeroservoelastic Semispan Model," *48th AIAA/ASME/ASCE/AHS/ASC Structural Dynamics, and Materials Conference*, No. AIAA-2007-1770, April 2007.

[3]Connolly, J., Kopasakis, G., and Lemon, K., "Turbofan Volume Dynamics Model for Investigations of Aero-Propulso-Servo-Elastic Effects in a Supersonic Commercial Transport," *46th AIAA/ASME/SAE/ASEE Joint Propulsion Conference and Exhibit*, No. AIAA-2009-4802, Aug. 2009.

[4]Kopasakis, G., Connolly, J., Paxson, D., and Ma, P., "Volume Dynamics Propulsion System Modeling for Supersonics Vehicle Research," *Journal of Turbomachinery*, Vol. 132, No. 4, October 2010, pp. 8.

[5]Kopasakis, G., "Atmospheric Turbulence Modeling," Tech. rep., NASA TM, 2010 Submitted for Publication.

[6]Kopasakis, G., "Feedback Control Systems Loop Shaping Design with Practical Considerations," Tech. rep., NASA TM 2007-215007, September 2007.

[7]Houpis, C., Rasmussen, S., and Sanz, M., *Quantitative Feedback Theory: Foundamentals and Applications*, Taylor Francis, 2006.

[8]Chavez, F. and Schmidt, D., "Analytical Aeropropulsive/Aeroelastic Hypersonic - Vehicle Model with Dynamic Analysis," *Journal of Guidance, Control, and Dynamics*, Vol. 17, No. 6, December 1994, pp. 1308–1319.

[9]Nguyen, N., "Integrated Flight Dynamic Modeling of Flexible Aircraft with Inertial Force-Propulsion-Aeroelastic Coupling," *44th AIAA Aerospace Sciences Meeting and Exhibit*, No. AIAA 2008-194, Reno, Nevada, 7-10 January 2008.

[10]Clark, A., Wu, C., Mirmirani, M., and Choi, S., "Development of an Airframe-Propulsion Integrated Generic Hypersonic Vehicle Model," *46th AIAA Aerospace Sciences Meeting and Exhibit*, No. AIAA 2006-218, Reno, Nevada, 9-12 January 2006.

[11]Pratt Whitney and General Electric, "Critical Propulsion Components: Inlet and Fan/Inlet Accoustics Team," Tech. rep., NASA CR-2005-213584, 2005.

[12]Saunders, J., "Two-Dimensional Bifurcated Inlet/Engine Tests Completed in 10 by 10 Foot Supersonic Wind Tunnel." http://www.grc.nasa.gov/WWW/RT/RT1998/5000/5850saunders.html., April 2009.

[13]Varner, M., Martindal, W., Phares, W., Kneile, K., and Adams, J., "Large Perturbation Flow Field Anaylsis and Simulation for Supersonic Inlet," Tech. rep., NASA CR-174676, 1985.

[14]Kopasakis, G. and Connolly, J., "Shock Positioning Controls Design for a Supersonic Inlet," *46th AIAA/ASME/SAE/ASEE Joint Propulsion Conference and Exhibit*, No. AIAA-2009-2803, Aug. 2009.

[15]Pratt Whitney and General Electric, "Critical Propulsion Components: Summary, Introduction, and Propulsion Systems Studies," Tech. rep., NASA CR-2005-213584, 2005.

[16]Seldner, K., Mihaloew, J., and Blaha, R., "Generalized Simulation Technique for Turbojet Engine System Analysis," Tech. rep., NASA TN-D-6610, 1972.

[17]Stueber, T. and Melcher, K., "J85 - 13 Turboject Engine Model for Propulsion System Control Studies," Tech. rep., NASA TP-2004-212223, 2004.

[18]Tesch, W. and Steenken, W., "Blade Row Dynamic Digital Compressor Program. Volume I: J85 Clean Inlet Flow and Parallel Compressor Models," Tech. rep., NASA CR-134978, 1976.

[19]Welch, P., "The Use of Fast Fourier Transform for the Estimation of Power Spectra: A Method Based on Time Averaging Over Short, Modified Periodograms," *IEEE Transactions Audio Electroacoustics*, Vol. AU, No. 15, 1967, pp. 70–73.

[20]Sugiyama, N., "Derivation of System Matrices from Nonlinear Dynamic Simulation of Jet Engines," *Journal of Guidance, Control, and Dynamics*, Vol. 17, No. 6, 1994.

[21]Kopasakis, G., "Modeling of Atmospheric Turblence as Disturbances for Control Design and Evaluation of High Speed Propulsion Systems," *Proceedings of ASME Turbo Expo 2010: Power for Land, Sea and Air*, No. GT2010-22851, Glasgow, UK, June 14-18 2010.

[22]Horowitz, I., "Quantitative Feedback Theory," *IEEE Proceedings*, Vol. 129, No. 6, Nov. 1982, pp. 215–226.

REPORT DOCUMENTATION PAGE			Form Approved OMB No. 0704-0188

1. REPORT DATE *(DD-MM-YYYY)*	2. REPORT TYPE	3. DATES COVERED *(From - To)*
01-10-2010	Technical Memorandum	

4. TITLE AND SUBTITLE
Loop Shaping Control Design for a Supersonic Propulsion System Model Using Quantitative Feedback Theory (QFT) Specifications and Bounds

5a. CONTRACT NUMBER

5b. GRANT NUMBER

5c. PROGRAM ELEMENT NUMBER

6. AUTHOR(S)
Connolly, Joseph, W.; Kopasakis, George

5d. PROJECT NUMBER

5e. TASK NUMBER

5f. WORK UNIT NUMBER
WBS 984754.02.07.03.20.02

7. PERFORMING ORGANIZATION NAME(S) AND ADDRESS(ES)
National Aeronautics and Space Administration
John H. Glenn Research Center at Lewis Field
Cleveland, Ohio 44135-3191

8. PERFORMING ORGANIZATION REPORT NUMBER
E-17476

9. SPONSORING/MONITORING AGENCY NAME(S) AND ADDRESS(ES)
National Aeronautics and Space Administration
Washington, DC 20546-0001

10. SPONSORING/MONITOR'S ACRONYM(S)
NASA

11. SPONSORING/MONITORING REPORT NUMBER
NASA/TM-2010-216897

12. DISTRIBUTION/AVAILABILITY STATEMENT
Unclassified-Unlimited
Subject Category: 07
Available electronically at http://gltrs.grc.nasa.gov
This publication is available from the NASA Center for AeroSpace Information, 443-757-5802

13. SUPPLEMENTARY NOTES

14. ABSTRACT
This paper covers the propulsion system component modeling and controls development of an integrated mixed compression inlet and turbojet engine that will be used for an overall vehicle Aero-Propulso-Servo-Elastic (APSE) model. Using previously created nonlinear component-level propulsion system models, a linear integrated propulsion system model and loop shaping control design have been developed. The design includes both inlet normal shock position control and jet engine rotor speed control for a potential supersonic commercial transport. A preliminary investigation of the impacts of the aero-elastic effects on the incoming flow field to the propulsion system are discussed, however, the focus here is on developing a methodology for the propulsion controls design that prevents unstart in the inlet and minimizes the thrust oscillation experienced by the vehicle. Quantitative Feedback Theory (QFT) specifications and bounds, and aspects of classical loop shaping are used in the control design process. Model uncertainty is incorporated in the design to address possible error in the system identification mapping of the nonlinear component models into the integrated linear model.

15. SUBJECT TERMS
Propulsion; Thrust; Control theory

16. SECURITY CLASSIFICATION OF:			17. LIMITATION OF ABSTRACT	18. NUMBER OF PAGES	19a. NAME OF RESPONSIBLE PERSON
a. REPORT	b. ABSTRACT	c. THIS PAGE			STI Help Desk (email:help@sti.nasa.gov)
U	U	U	UU	24	19b. TELEPHONE NUMBER *(include area code)* 443-757-5802